FEMS Microbiology Ecology, 97, 2021, fiab124

https://doi.org/10.1093/femsec/fiab124
Advance Access Publication Date: 1 September 2021
Research Article

RESEARCH ARTICLE

Nitrate-dependent anaerobic methane oxidation and chemolithotrophic denitrification in a temperate eutrophic lake

Fleur A. E. Roland[1,*,†], Alberto V. Borges[1], Steven Bouillon[2] and Cédric Morana[1]

[1]Chemical Oceanography Unit, Université de Liège, 4000 Liège, Belgium and [2]Department of Earth and Environmental Sciences, Katholieke Universiteit Leuven (KU Leuven), 3001 Leuven, Belgium

*Corresponding author: 19, Allée du 6 Août, 4000 Liège, Belgium. Tel: +323663326; E-mail: froland@uliege.be

One sentence summary: Biogeochemical processes measurements highlight the occurrence of complex interactions between carbon, nitrogen and sulfur cycles in the water column of a permanently stratified European lake.

Editor: Martin W. Hahn

†Fleur A. E. Roland, https://orcid.org/0000-0002-3624-0001

ABSTRACT

While the emissions of methane (CH_4) by natural systems have been widely investigated, CH_4 aquatic sinks are still poorly constrained. Here, we investigated the CH_4 cycle and its interactions with nitrogen (N), iron (Fe) and manganese (Mn) cycles in the oxic-anoxic interface and deep anoxic waters of a small, meromictic and eutrophic lake, during two summertime sampling campaigns. Anaerobic CH_4 oxidation (AOM) was measured from the temporal decrease of CH_4 concentrations, with the addition of three potential electron acceptors (NO_3^-, iron oxides ($Fe(OH)_3$) and manganese oxides (MnO_2)). Experiments with the addition of either ^{15}N-labeled nitrate ($^{15}N\text{-}NO_3^-$) or $^{15}N\text{-}NO_3^-$ combined with sulfide (H_2S), to measure denitrification, chemolithotrophic denitrification and anaerobic ammonium oxidation (anammox) rates, were also performed. Measurements showed AOM rates up to 3.8 μmol CH_4 L^{-1} d^{-1} that strongly increased with the addition of NO_3^- and moderately increased with the addition of $Fe(OH)_3$. No stimulation was observed with MnO_2 added. Potential denitrification and anammox rates up to 63 and 0.27 μmol N_2 L^{-1} d^{-1}, respectively, were measured when only $^{15}N\text{-}NO_3^-$ was added. When H_2S was added, both denitrification and anammox rates increased. Altogether, these results suggest that prokaryote communities in the redoxcline are able to efficiently use the most available substrates.

Keywords: anaerobic methane oxidation; nitrate; iron; manganese; denitrification; anammox

INTRODUCTION

The Paris Agreement ratified in 2016 states that the global average temperature must be kept below 1.5°C compared with the pre-industrial period to limit the consequences of global warming. With this perspective, methane (CH_4) plays a key role, since its global warming potential is 28 times higher on a 100-year time frame than carbon dioxide (CO_2) but has a much shorter residence time in the atmosphere than CO_2 (IPCC 2014). The atmospheric CH_4 concentrations have dramatically increased compared with the pre-industrial era because huge amounts of CH_4 are annually released into the atmosphere (~8 $GtCO_{2eq}$ yr^{-1}), 50–65% being from anthropogenic sources (mainly agriculture, waste, fossil fuel production and use) (IPCC 2014), and the remaining 35–50% being produced by natural systems, among which lakes contribute ~10% (Saunois *et al.* 2016, 2020).

Received: 9 February 2021; **Accepted:** 30 August 2021

© The Author(s) 2021. Published by Oxford University Press on behalf of FEMS. All rights reserved. For permissions, please e-mail: journals.permissions@oup.com

Downloaded from https://academic.oup.com/femsec/article/97/10/fiab124/6360975 by University of Liege user on 17 September 2021

While a notable effort has been made to quantify global sources of CH_4 from natural environments, aquatic CH_4 sinks have been less investigated. In aquatic systems, CH_4 is mainly produced in anoxic sediments by methanogenic archaea, and is then emitted via diffusion or ebullition in the water column. A large part of the CH_4 produced is biologically oxidized by aerobic or anaerobic methanotrophs before reaching the atmosphere (Borrel *et al.* 2011). Anaerobic methane oxidation (AOM) can be coupled to different electron acceptors: sulfate (SO_4^{2-}), nitrate (NO_3^-), nitrite (NO_2^-), iron (Fe) oxides or manganese (Mn) oxides (Borrel *et al.* 2011). More recently, it has also been suggested that AOM could occur with organic compounds (Valenzuela *et al.* 2017; Bai *et al.* 2019). It was initially thought that AOM was exclusively performed by a consortium of archaea (ANME-type) and SO_4^{2-}, NO_3^-, NO_2^-, Fe or Mn reducers (Knittel and Boetius 2009; Cabrol *et al.* 2020), but it was recently demonstrated that bacteria from the phylum NC10 were also capable to perform AOM coupled to NO_2^- reduction without any partner (Ettwig *et al.* 2010; Oswald *et al.* 2017; Graf *et al.* 2018). Besides, some studies also suggested that AOM could be performed by aerobic methanotrophs, in micro-oxic conditions (Blees *et al.* 2014; Oswald *et al.* 2016b), or also that some Archaea were capable of decoupling AOM and SO_4^{2-} reduction (Scheller *et al.* 2016). Sulfate-dependent AOM is mainly encountered in marine environments (Reeburgh 2007) due to higher SO_4^{2-} concentrations in seawater, but has also been shown in freshwaters (Eller, Känel and Krüger 2005; Schubert *et al.* 2011; Roland *et al.* 2017, 2018b). In freshwaters, the other potential electron acceptors can be found in higher concentrations, and are thus assumed to contribute more significantly to AOM (e.g. Borrel *et al.* 2011; Crowe *et al.* 2011; Sturm *et al.* 2016). Humic substances have also been found to fuel anaerobic methane oxidation in humic-rich freshwater ecosystems, such as wetlands (Valenzuela *et al.* 2020).

The occurrence of AOM coupled to the reduction of Fe or Mn oxides is thermodynamically favorable, and has been envisaged in lakes (Crowe *et al.* 2011; Sivan *et al.* 2011; á Norði *et al.* 2013; Sturm *et al.* 2019) and in marine sediments (Beal, House and Orphan 2009; Cui *et al.* 2015; Egger *et al.* 2015), but its natural significance and its mode of action remain poorly understood due to the complexity of natural environments in which multiple electron acceptors are present. A certain discrepancy appears in the literature, AOM sometimes being stimulated by the addition of minerals, and sometimes not (Oswald *et al.* 2016b; Bar-Or *et al.* 2017; Rissanen *et al.* 2017). NO_3^-- or NO_2^--dependent AOM (DAMO) is more documented (e.g. Raghoebarsing *et al.* 2006; Ettwig *et al.* 2009, 2010; Deutzmann and Schink 2011; Kits, Klotz and Stein 2015; Oswald *et al.* 2017), but direct in-situ measurements of the process have seldom been reported in the literature. DAMO is thermodynamically more favorable than SO_4^{2-}-dependent AOM, and can thus potentially play a key role in the reduction of CH_4 emissions from freshwaters (Raghoebarsing *et al.* 2006). However, it may also compete with heterotrophic denitrification (NO_3^- reduction with organic matter as electron donor, performed by a variety of prokaryotes, including *Bacillus*, *Paracoccus* and *Pseudomonas*; Bernhard 2010) and anaerobic ammonium oxidation (anammox; NO_3^- or NO_2^- reduction coupled to ammonium oxidation, performed by bacteria belonging to the phylum Planctomycetes; Bernhard 2010) for substrates, two thermodynamically more favorable processes, commonly encountered in anoxic environments. The balance between the different biotic processes for access to the substrates plays a key role in the occurrence of AOM.

We previously showed that AOM occurred in a temperate, eutrophic and meromictic stone pit lake (Lake Dendre, Belgium; Roland *et al.* 2017). Lake Dendre is considered as meromictic, the water column remaining anoxic below 20-m depth throughout the year. The epilimnion shows strong seasonal variability, with waters anoxic from 10-m depth in summer, while it is entirely mixed (up to 20-m depth) in winter. The lake is characterized by high SO_4^{2-} concentrations all along the vertical profile (up to ~1500 μmol L^{-1}), high CH_4 and sulfide (H_2S) concentrations in anoxic waters (up to ~1000 and ~100 μmol L^{-1}, respectively), and by an underwater spring located at 17-m depth (in the anoxic compartment), delivering substantial quantities of NO_3^- (up to ~80 μmol L^{-1}) due to generalized fertilizer contamination of groundwater in Belgium (SPW-DGO3 2021; Roland *et al.* 2017). In our previous study (Roland *et al.* 2017), we suggested that AOM was mainly coupled to SO_4^{2-} reduction, given the overall high SO_4^{2-} concentration throughout the entire water column. However, we also showed that NO_3^-, Fe and Mn concentrations in the water column of Lake Dendre were not negligible, and a concomitance between maximum AOM peaks and maximum NO_3^- concentration peaks was observed (Roland *et al.* 2017). We hypothesize that the underwater spring could provide the N substrate to sustain elevated denitrification and NO_3^--dependent AOM rates in anoxic waters. During this study, we thus investigated alternative pathways of AOM, by conducting incubations with addition of the different potential electron acceptors NO_3^-, Fe oxides and Mn oxides, as well as measurements of denitrification, to check for the occurrence of DAMO and potentially competitive relationships.

MATERIALS AND METHODS

Physico-chemical parameters and sampling

Sampling in the Dendre stone pit lake (50.6157°N, 3.7949°E; Wallonia, Belgium) was carried out during the summers of 2017 and 2018. Depth profiles of dissolved oxygen (O_2) concentrations, temperature, pH and specific conductivity were obtained with a YSI Exo multiparameter probe (YSI, Yellow Spring, Ohio, USA). The conductivity, pH and oxygen sensors were calibrated the day before each sampling using the protocols and standards recommended by the manufacturer (YSI). Sampling of water for the different measurements was performed with a Niskin bottle (General Oceanics, Miami, Florida, USA) through a silicon tube connected to the outlet. All the samples were left to overflow the vial volume three times before sealing.

CH_4, CO_2 and N_2O concentration profiles

Duplicate samples for N_2O and CH_4 concentration analyses were collected in 60-mL glass serum bottles (Derco, Ittre, Belgium), which were immediately sealed with butyl stoppers (Wheaton, Milville, New Jersey, USA) and aluminium caps (Wheaton, Milville, New Jersey, USA). In 2017, water was sampled in oxic waters at 1-, 4- and 7-m depths, at the oxic-anoxic interface at 9-, 10- and 11-m depths and in the anoxic waters at 13-, 15-, 17- and 20-m depths. In 2018, sampling for determination of the vertical profiles of dissolved gases was carried out at 1-, 7-, 10-, 13-, 15- and 17-m depths.

CH_4 and N_2O concentrations were determined via the headspace equilibration technique (20-mL N_2 headspace in 60-mL serum bottles) and measured by gas chromatography (GC) with electron capture detection (ECD) for N_2O and with flame ionization detection (FID) for CH_4 (Weiss 1981). The SRI 8610C GC-ECD-FID (SRI, Torrance, California, USA) was calibrated with certified CH_4: CO_2: N_2O: N_2 mixtures (Air Liquide, Liège, Belgium)

Downloaded from https://academic.oup.com/femsec/article/97/10/fiab124/6360975 by University of Liege user on 17 September 2021

of 1, 10, 30 and 509 ppm CH_4 and of 0.2, 2.0 and 6.0 ppm N_2O. Concentrations were computed using the solubility coefficients of Yamamoto, Alcauskas and Crozier (1976) and Weiss and Price (1980), for CH_4 and N_2O, respectively. The precision of measurements was ±3.9% and ±3.2% for CH_4 and N_2O, respectively.

Triplicate samples for determination of the partial pressure of CO_2 (pCO_2) were collected in 60-mL plastic syringes directly from the Niskin, at the same depths as the CH_4 and N_2O vertical profiles in 2017, and at 1-, 5-, 7-, 10-, 13-, 15-, 17- and 19-m depths in 2018. The pCO_2 was measured with an infra-red gas analyzer (Licor Li-840, Lincoln, Nebraska, USA) after headspace equilibration in the syringe (Abril *et al.* 2015; Borges *et al.* 2015). The Li-840 was calibrated with N_2 and certified CO_2: N_2 mixtures (Air Liquide, Liège, Belgium) of 388, 813, 3788 and 8300 ppm CO_2. The precision of measurements was ±4.1%.

Dissolved inorganic nitrogen species and major element concentrations

Water from the water column was collected for the determination of nitrogen nutrients (NO_3^-, NO_2^- and NH_4^+) and major element concentrations along the vertical profiles (the same depths as the dissolved gases' vertical profiles). NO_2^- and NO_3^- concentrations were determined using the sulfanilamide colorimetric method, and NH_4^+ with the dichloroisocyanurate-salicylate-nitroprussiate colorimetric method (Westwood 1981; APHA 1998). They were determined colorimetrically using a 5-cm optical path, with a Genesys 10 vis spectrophotometer (Thermo Fisher Scientific, Waltham, Massachusetts, USA). The detection limits of the methods were 0.15, 0.03 and 0.3 μmol L^{-1} for NO_3^-, NO_2^- and NH_4^+, respectively.

Samples for determination of major elements (Fe and Mn) were taken at the same depths as the nutrients and dissolved gases, were stored in 20-mL scintillation vials and preserved with 50 μL of HNO_3 (65%, Suprapur grade, Sigma-Aldrich, Saint-Louis, Missouri, USA). Dissolved Mn, Fe and S concentrations were measured with inductively coupled plasma MS (ICP-MS; Agilent 7700x, Santa Clara, California, USA) calibrated with the following standards: SRM1640a from National Institute of Standards and Technology (Gaithersburg, Maryland, USA), TM27.3 (lot 0412) and TMRain-04 (lot 0913) from Environment Canada (Québec, Canada) and SPS-SW2 Batch 130 from Spectrapure Standard (Spectrapure, Tempe, Arizona, USA). The limits of quantification were 46.97, 0.002 and 0.01 μmol L^{-1} for S, Mn and Fe, respectively. Due to a problem with sample preservation in 2018, major elements are only available for the field campaign of 2017.

CH_4 oxidation measurements (sampling of 2018)

Depths for CH_4 oxidation measurement were chosen based upon previous field campaigns (Roland *et al.* 2017), at the oxic-anoxic interface (10-m depth) and below (13- and 17-m depths) in the water layer under the influence of the external source bringing NO_3^- into the anoxic waters and penetrating the lake at a depth of 17 m.

Samples for determination of the CH_4 oxidation rates were collected in 60-mL glass serum bottles and immediately sealed with butyl stoppers and aluminum caps. Two samples per depth were immediately poisoned with 200 μL of a saturated $HgCl_2$ solution (VWR, Leuven, Belgium) (T0) to subsequently determine the initial CH_4 concentrations at the beginning of the incubation, and four unmanipulated bottles (control treatment) were incubated in the dark and at constant temperature (close to in-situ temperature, so 20°C on the surface, 10°C in the redox zone and 5°C below a depth of 10 m). The biological activity in the incubation bottles was stopped at different time intervals (~20, 45, 75 and 90 h) by the addition of 200 μL of a saturated $HgCl_2$ solution. They were then stored in the dark until analysis in the laboratory following the method described above for CH_4 concentration determination.

Sixteen supplementary samples were incubated under the same conditions but were amended by the addition of different electron acceptors after a pre-incubation period of 12 h, to remove oxygen potentially inadvertently introduced during sampling. Four of them received 100 μL of a solution of nitrate KNO_3 (12 g L^{-1}, final concentration of 200 μmol L^{-1}), four received 100 μL of the same solution of nitrate plus 100 μL of a solution of H_2S (60 g L^{-1}, final concentration of 100 μmol L^{-1}), four received 100 μL of a solution of Fe_2O_3 (4.8 g L^{-1}, final concentration of 50 μmol L^{-1}) and four received 100 μL of a solution of MnO_2 (2.6 g L^{-1}, final concentration of 50 μmol L^{-1}). The concentrations of the different solutions were chosen to be in excess compared with the natural concentrations. The different electron acceptor solutions (except those with H_2S) were stored in 30-ml sealed glass serum bottles and flushed with helium for 10 min to evacuate atmospheric oxygen that had potentially been inadvertently introduced. To avoid any trace oxygen contamination during the injection of the electron acceptor solution, all bottles remained closed and solutions were taken with a syringe and a needle through the septum and injected into the different samples, also through the septum.

The biological activity in the incubation bottles was stopped after the same time interval and following the same method as in the control treatment described above. They were then stored in the dark until analysis in the laboratory following the method described above for CH_4 concentration determination.

CH_4 oxidation rates were estimated as the slope of the linear regression of CH_4 concentration (μmol L^{-1}) versus time during the incubation (per day). CH_4 oxidation was considered significant only if the slope of the linear regression was significantly lower than 0 (95% confidence interval). Oxidation rates in the experiments with the addition of different potential electron acceptors were considered as moderately stimulated when the slope in the treatment was higher than 1 standard deviation of the slope of the control (confidence interval of 68%, 1 σ), or strongly stimulated when it was higher than 2 standard deviations (confidence interval of 95%, 2 σ). Statistical testing was performed using Graphpad Prism 7 Software.

CH_4 emissions calculations

CH_4 emissions to the atmosphere were calculated as described by Roland *et al.* (2017). Briefly, the CH_4 concentration gradient across the air-water interface was computed from the CH_4 concentration at a depth of 1 m, and the gas transfer velocity was computed from wind speed according to the Cole and Caraco (1998) relationship. A positive emission value corresponds to a net gas transfer from the water to the atmosphere.

Anammox and denitrification rates measurements

Sampling of 2017

Denitrification measurements were performed at six depths (9, 10, 11, 13, 15 and 17 m), located at the oxic-anoxic interface and below the water layer under the influence of the external source

Downloaded from https://academic.oup.com/femsec/article/97/10/fiab124/6360975 by University of Liege user on 17 September 2021

that brings NO_3^- into the anoxic waters, and where H_2S concentrations are high.

For each depth, two 250-mL glass serum bottles were filled directly from the tubing of the Niskin bottle taking care to avoid air bubbles and were immediately closed without headspace. These bottles were pre-incubated for 12 h before further manipulation, for the same reasons as described above. After the pre-incubation period, the bottles were spiked with tracer solutions following two different treatments: (i) addition of a solution of $K^{15}NO_3^-$ (Eurisotop, Saint-Aubin, France) (final concentration of 100 μmol L^{-1}), and (ii) addition of the same solution of $K^{15}NO_3^-$ and with a solution of dissolved H_2S (Sigma-Aldrich, Saint-Louis, Missouri, USA) (final concentration of 100 μmol L^{-1}) in order to test the effect of H_2S addition on the denitrification process. Given the fact that all the tracer and H_2S molecules were added in excess, we considered that measured rates should be viewed as potential rates.

After the tracer addition, the water samples contained in each of the 250-ml serum bottles were gently transferred into 12-mL Exetainer glass vials (Labco, Lampeter, UK) with a syringe and silicone tubing. Six Exetainer vials per 250-ml bottle were overfilled and closed without headspace. One Exetainer vial was immediately stopped (T0 sample) by injection of 500 μL of 20% zinc acetate (ZnAc; VWR, Leuven, Belgium); the others were placed in the dark at a temperature close to the *in situ* temperature and were stopped after 6, 12, 18, 24 and 48 h of incubation. Exetainer vials for denitrification and anammox rates measurement were stored in the dark until quantification of the $^{29}N_2$ and $^{30}N_2$ with an elemental analyzer-isotope mass spectrometer (EA-IRMS, EA1112 coupled to deltaV advantage; Thermo Fisher Scientific, Waltham, Massachusetts, USA) after creating a 2-ml helium headspace. Denitrification and anammox rates were calculated according to Equations 1 and 2 (Thamdrup and Dalsgaard 2002; Thamdrup *et al.* 2006):

$$N_2\ \text{denitrification} = {}^{15}N^{15}N_{excess} * (F_{NO3})^{-2} \quad (1)$$

$$N_2\ \text{anammox} = (F_{NO3})^{-1} * \left({}^{14}N^{15}N_{excess} + 2 * \left(1 - (F_{NO3})^{-1}\right) * {}^{15}N^{15}N_{excess}\right) \quad (2)$$

where N_2 denitrification and N_2 anammox are the production of N_2 by denitrification and anammox, respectively, $^{15}N^{15}N_{excess}$ and $^{14}N^{15}N_{excess}$ are the production of excess $^{15}N^{15}N$ and $^{14}N^{15}N$, respectively, and F_{NO3} is the fraction of $^{15}NO_3^-$ in the NO_3^- pool ($^{15}NO_3^-/(^{15}NO_3^- + NO_3^-)$). $^{15}N^{15}N$ and $^{14}N^{15}N$ excess is the excess relative to masses of 30 and 29, respectively, in the T0 samples. The limit of detection for denitrification and anammox measurements with the above mentioned IRMS setup was estimated based on triplicate injection of a selection of samples and was 10.4 nmol L^{-1} d^{-1} for denitrification and 6.1 nmol L^{-1} d^{-1} for anammox.

Natural denitrification rates can be deduced from potential rates using the following equation (Thamdrup *et al.* 2006):

$$\text{Natural } N_2 \text{ denitrification} = \text{Potential } N_2 \text{ denitrification} * (1 - F_{NO3}) \quad (3)$$

where natural N_2 denitrification is the natural production of N_2 by denitrification, potential N_2 denitrification is the potential denitrification rate (as described in Equation 1) and F_{NO3} is the fraction of $^{15}NO_3$ in the NO_3^- pool.

Sampling of 2018

Denitrification measurements were performed at four depths (13, 15, 17 and 19 m) with the same general procedure as described above, but water samples were incubated following the following treatments: (i) 250-ml serum bottles were spiked with a solution of $K^{15}NO_3^-$ (final concentration of 200 μmol L^{-1}), or (ii) with a solution of $^{15}NH_4Cl$ (Eurisotop, Saint-Aubin, France) (final concentration of 200 μmol L^{-1}) and a solution of $K^{14}NO_3^-$ (final concentration of 200 μmol L^{-1}) to specifically target the anammox process. After the tracer addition, Exetainer vials were filled, poisoned and processed in the laboratory as described above. Anammox rates were calculated as follows:

$$N_{2\ \text{anammox}\ 15NH4} = {}^{15}N^{14}N_{excess} * (F_{NH4})^{-1} \quad (4)$$

where $N_{2\ \text{anammox}\ 15NH4}$ is the production of N_2 by anammox in the treatment with $^{15}NH_4^+$ added, $^{15}N^{14}N_{excess}$ is the production of excess $^{15}N^{14}N$ and F_{NH4} is the fraction of $^{15}NH_4^+$ in the NH_4^+ pool ($^{15}NH_4^+/(^{15}NH_4^+ + NH_4^+)$).

RESULTS

Chemical composition and seasonal variability of the water column

Differences occurred in the physico-chemical vertical profiles from 2017 to 2018 (summer 2018 was characterized by very high air temperatures and a severe drought across Europe) (Fig. 1). An offset in the thermocline, chemocline and oxycline positions could be observed, with deeper clines in 2018. O_2 concentrations at the surface were typically around 11 mg L^{-1} during both field campaigns, and the water column was anoxic (O_2 below detection limit) from a 10-m depth in 2017 and from a 12-m depth in 2018. A peak of higher O_2 concentrations (up to 14 mg L^{-1}) was observed in 2018 at the bottom of the epilimnion and photic zone (8-m depth) and related to higher chlrorophyll-*a* content (Fig. S1).

A wide NO_3^- and NO_2^- accumulation zone spreading almost through the entire oxycline and the upper part of the anoxic compartment was observed in 2017 (Fig. 2), with concentrations peaking right at the oxic-anoxic transition for NO_3^- (33 μmol L^{-1} at 10 m) and slightly below for NO_2^- (20 μmol L^{-1} at 11 m). This accumulation zone extended in the anoxic compartment down to 15 m. NO_3^- and NO_2^- concentrations were much lower in 2018, with a maximum of 9 μmol L^{-1} and less than 0.5 μmol L^{-1} for NO_3^- and NO_2^-, respectively. In contrast to 2017, no distinct accumulation zone could be observed. NH_4^+ shows an opposite pattern, with an increase in concentration with depth in the anoxic compartment, particularly abrupt at the bottom of the NO_3^- and NO_2^- accumulation zone in 2017. N_2O maximum concentration peaks of 29 and 55 nmol L^{-1} (in 2017 and 2018, respectively) were observed in oxic waters, while peaks of 17 and 8 nmol L^{-1} (in 2017 and 2018, respectively) were also observed in anoxic waters.

Total Fe concentrations were low throughout the water column, with maximum concentrations of 0.8 μmol L^{-1} observed in oxic waters. Total Mn concentrations were higher, and sharply increased in anoxic waters, up to ~15 μmol L^{-1}. The water column was very rich in S, with concentrations of up to ~650 μmol L^{-1}.

CH_4 and pCO_2 vertical profiles showed similar patterns during both sampling campaigns, with a first increase of pCO_2 with depth starting in the thermocline, below the photic zone (~5 m), and a second in the conductivity gradient between 15 and 20 m. CH_4 concentrations gradually increased with depth in the anoxic compartment, below the oxic-anoxic transition. The lake was a net source of CH_4 during both sampling campaigns, with emis-

Downloaded from https://academic.oup.com/femsec/article/97/10/fiab124/6360975 by University of Liege user on 17 September 2021

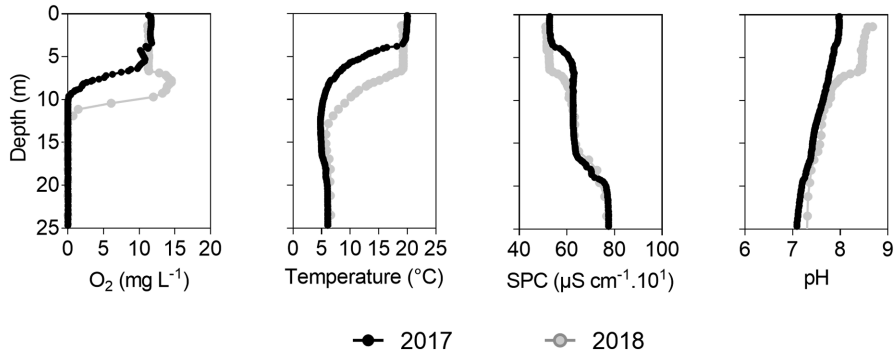

Figure 1. Physico-chemical parameters (oxygen concentrations (mg L^{-1}), temperature (°C), specific conductivity (SPC, µS $cm^{-1}.10^1$) and pH) in Lake Dendre in 2017 (black) and 2018 (gray).

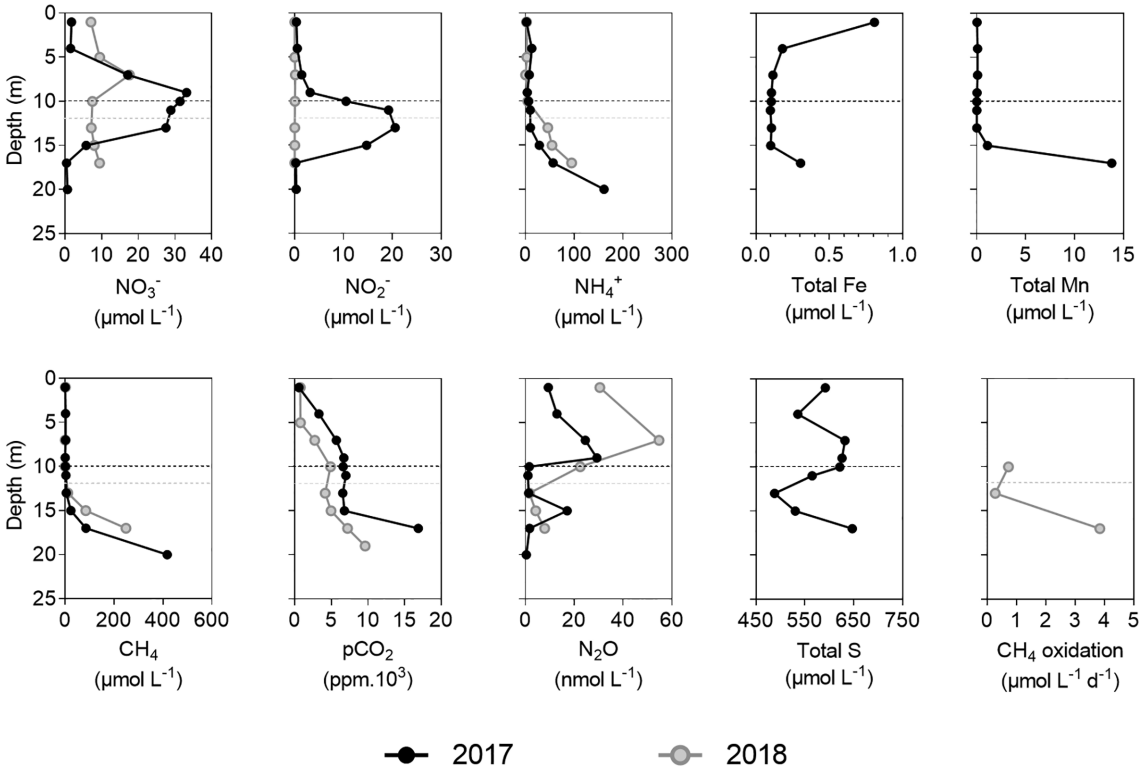

Figure 2. Vertical profiles of nitrogenous nutrients (NO_3^-, NO_2^-, NH_4^+), major elements (total Fe, Mn, S) and dissolved gases (CH_4, pCO_2, N_2O) concentrations during both sampling campaigns, and CH_4 oxidation, in 2018. Horizontal dashed lines represent the respective oxic-anoxic interfaces for each sampling campaign. Black: 2017; gray: 2018.

sion rates estimated at 0.64 and 0.55 mmol m^{-2} d^{-1} in 2017 and 2018, respectively.

CH_4 oxidation

The maximum of CH_4 oxidation (MOX) measured in control (unmanipulated) samples was located well below the oxic-anoxic transition zone (located at 12 m), with a maximum rate of 3.84 µmol CH_4 L^{-1} d^{-1} measured at a depth of 17 m (Figs 2 and S2). The experiment with addition of potential electron acceptors showed that MOX was moderately stimulated by the addition of NO_3^- and Fe oxides at 10 and 13 m (except Fe), and was strongly stimulated at 17 m (Fig. 3, Supplemental Table 1). By contrast, Mn addition did not significantly affect the CH_4 oxidation rates, which were even lower than in the control samples at depths of 13 and 17 m.

Denitrification and anammox

Potential denitrification rates were modest in the upper part of the hypolimnion but abruptly increased at depths below 15 m, with maximum rates measured at 17 m during both sampling cruises (up to 17 and 63 µmol N_2 L^{-1} d^{-1} in 2017 and 2018, respectively) (Figs 4, S2 and S4), slightly below the lower limit of the NO_3^- and NO_2^- accumulation zone (Fig. 2). Significant potential anammox rates (up to 0.27 µmol N_2 L^{-1} d^{-1}) were only detected in 2017, with two maximum peaks at depths of 11 and 15 m, but did not follow any clear vertical pattern.

In 2017, denitrification was significantly stimulated by the addition of H_2S (up to 1470 times increase) at every depth (Fig. 5), with the exception of 17-m depth, where ambient H_2S concentrations were already high. H_2S also enhanced anammox between 9 and 11 m (up to 152 times increase).

Downloaded from https://academic.oup.com/femsec/article/97/10/fiab124/6360975 by University of Liege user on 17 September 2021

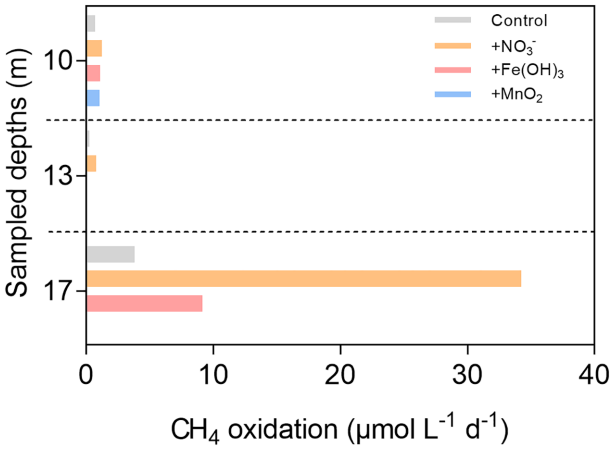

Figure 3. Methane oxidation rates in the control incubations (gray), and in incubations with the different potential electron acceptors added (light orange: NO_3^-; red: Fe oxides; blue: Mn oxides), during the sampling campaign of 2018.

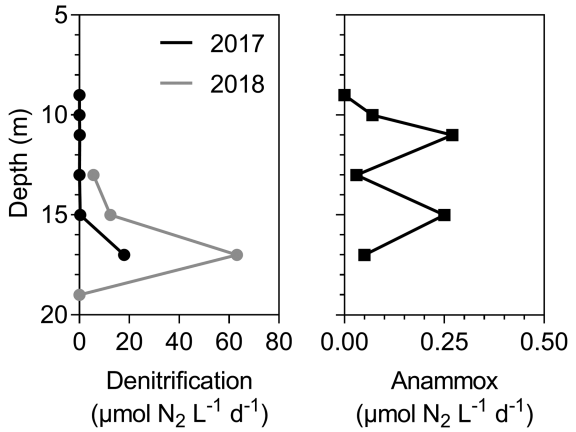

Figure 4. Vertical profiles of denitrification (circles) and anammox (squares) rates (µmol N_2 L^{-1} d^{-1}) in 2017 (black) and 2018 (gray). Note that anammox was not observed in 2018.

Maximum natural denitrification rates observed were estimated at 2.9 µmol N_2 L^{-1} d^{-1}.

DISCUSSION

An active N cycle

An active N cycle was observed in the water column, with substantial denitrification (in 2017 and 2018) and anammox (in 2017 only) rates observed in anoxic waters. Furthermore, the vertical profiles of NH_4^+, NO_3^- and NO_2^-, with a decrease of NH_4^+ at the oxic-anoxic interface and an accumulation of NO_3^- and NO_2^- in the oxycline (below the photic zone) and in the upper part of anoxic compartment, provide indirect evidence for the occurrence of active nitrification in the water column of Lake Dendre at the oxic-anoxic interface. This is supported by the observation of N_2O concentration maxima in the oxycline, which could be linked to nitrifier activity (e.g. Barnard, Leadley and Hungate 2005; Kirchman *et al.* 2008; Ji *et al.* 2015; Battaglia and Joos 2018).

While heterotrophic denitrification is usually assumed to be ubiquitous in anoxic waters and sediments of freshwater ecosystems, observations of alternative denitrification pathways using inorganic electron donors such as H_2S (chemoautotrophic denitrification) have been mostly restricted to marine sediments, or in the oxygen minimum zone of several marine basins such as the Baltic Sea (Labrenz *et al.* 2005), Black Sea (Brettar and Rheinheimer 1991) or the coastal upwelling off Chile (Galán *et al.* 2014). This could be related to the fact that freshwater systems usually harbor lower sulfate (and then sulfide) but higher organic matter concentrations in comparison with marine systems (Capone and Kiene 1988). Notable exceptions are sulfide-rich, deep meromictic lakes such as Lake Kivu (Roland *et al.* 2018b) or Lake Lugano (Wenk *et al.* 2013), where co-occurrence of anammox and sulfide-dependent denitrifiers was reported. Similar to Lake Cadagno, our results showed that potential denitrification was strongly stimulated by H_2S addition at every depth from the oxic-anoxic interface down to 17 m, where ambient H_2S concentrations usually increase (Roland *et al.* 2017), suggesting electron donor limitation of sulfide-dependent denitrification in Lake Dendre. Potential denitrification was not only detected in the nitrogenous compound accumulation zone, but also deeper, down to 17 m. This pattern might be explained by lateral intrusion of NO_3^--rich groundwater (Borges *et al.* 2018) fed by a sub lacustrine spring located at a depth of ~17 m. Anammox activity was detected in 2017 and was also stimulated by H_2S addition, although to a much lesser extent than denitrification. Reports on the effects of H_2S on anammox activity are contradictory, with some showing that they can be inhibited in the presence of H_2S (Dalsgaard *et al.* 2003; Jensen *et al.* 2008, 2009), and others showing that they could actually even be stimulated by external H_2S supply (Wenk *et al.* 2013; Roland *et al.* 2018a; Qin *et al.* 2019). Our observations are similar to those of Wenk *et al.* (2013), who suggested that in Lake Lugano anammox might rely on the NO_2^- produced as an intermediate of sulfide-dependent denitrification and benefit from a locally detoxified environment (removal of H_2S by sulfide-dependent denitrifiers) if organized in aggregate with sulfide-dependent denitrifiers.

While potential anammox rates measured in Lake Dendre during this study were similar to other sites in the literature (Table 1), higher potential denitrification rates were observed. Denitrification being dependent on the trophic status (Bai *et al.* 2019), the high denitrification rates observed can be linked to the eutrophic status of Lake Dendre and the continuous supply of NO_3^--rich waters to the anoxic compartment by a sub lacustrine spring. The maximum potential sulfide-dependent denitrification measured in Lake Dendre (57 µmol N_2 L^{-1} d^{-1}) was also much higher than in Lake Lugano (0.2 µmol N_2 L^{-1} d^{-1}), and might be related to the overall higher electron donors availability (H_2S) found in Lake Dendre (up to 100 and 12 µmol L^{-1} in Lake Dendre and Lugano, respectively; Wenk *et al.* 2013; Roland *et al.* 2017b).

CH_4 biogeochemistry in anoxic waters

The CH_4 oxidation rates measured in the control treatment (without any amendment, so occurring with natural substrates, such as SO_4^{2-} present at very high concentrations; Roland *et al.* 2017b) were significantly lower than the maximum oxidation rate of 15 µmol L^{-1} d^{-1} reported in Lake Dendre during our previous research (Roland *et al.* 2017), suggesting a strong seasonal and inter-annual variability. Regarding anaerobic oxidation rates reported in the literature, a strong spatial variability is observed between study sites (Table 1), and rates are strongly influenced by natural CH_4 concentrations of the environment (Fig. 6), except for Lake Matano and Lake Pavin, which presented higher oxidation rates for moderate CH_4 concentrations and lower oxidation rates for higher CH_4 concentrations, respectively (Lopes *et al.* 2011; Sturm *et al.* 2019). In Lake Dendre, the pattern is less clear,

Downloaded from https://academic.oup.com/femsec/article/97/10/fiab124/6360975 by University of Liege user on 17 September 2021

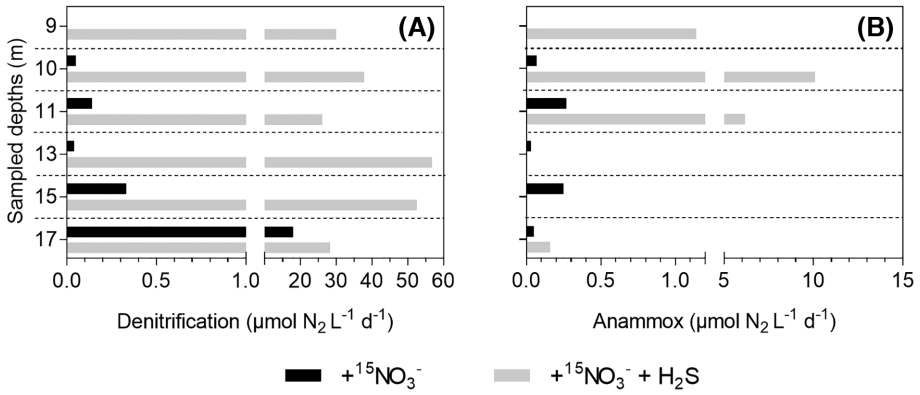

Figure 5. (**A**) Denitrification rates (µmol N_2 L^{-1} d^{-1}) and (**B**) anammox rates (µmol N_2 L^{-1} d^{-1}), measured in incubations with $^{15}N\text{-}NO_3^-$ (black) and $^{15}N\text{-}NO_3^- + H_2S$ (gray), during the campaign of 2017.

Table 1. Denitrification, anammox and anaerobic methane oxidation (AOM) rates (µmol N_2 L^{-1} d^{-1} and µmol CH_4 L^{-1} d^{-1}, respectively) in the water column of different aquatic environments (see Supplemental Table 2 for the hydro-morphological characteristics of each environment).

	Maximum rates (µmol L^{-1} d^{-1})	Source
Potential denitrification		
Lake Dendre	63.2	This study
Baltic Sea	1.2	Dalsgaard, De Brabandere and Hall Per (2013)
Lake Kivu (Africa)	4.2	Roland *et al.* (2018a)
Lake Tanganyika (Africa)	1.2	Schubert *et al.* (2006)
Lake Erie (North America)	0.4	Lu *et al.* (2018)
Potential anammox		
Lake Dendre	0.3	This study
Lake Kivu (Africa)	0.2	Roland *et al.* (2018a)
Lake Tanganyika (Africa)	0.2	Schubert *et al.* (2006)
Golfo Dulce	0.5	Dalsgaard *et al.* (2003)
Benguela upwelling system	0.2	Kuypers *et al.* (2005)
Lake Erie (North America)	0.9	Lu *et al.* (2018)
AOM		
Lake Dendre	3.8	This study
Lake Dendre	15	Roland *et al.* (2017)
Lake Kivu (Africa)	16	Roland *et al.* (2018b)
Lake Pavin (France)	0.4	Lopes *et al.* (2011)
Lake Marn (Sweden)	2.2	Bastviken, Ejlertsson and Tranvik (2002)
Lake Illersjoen (Sweden)	3	Bastviken, Ejlertsson and Tranvik (2002)
Lake Big Soda (USA)	0.01	Iversen, Oremland and Klug (1987)
Lake Matano (Indonesia)	181	Sturm *et al.* (2019)
Lake Tanganyika (Africa)	1.8	Rudd, Hamilton and Campbell (1974)
Lake Paul (USA)	5.6	Bastviken *et al.* (2008)
Lake Peter (USA)	6.3	Bastviken *et al.* (2008)
Lake Hummingbird (USA)	2.4	Bastviken *et al.* (2008

suggesting that CH_4 concentrations are not the main and/or only factor determining the magnitude of CH_4 oxidation.

Experiments with the addition of three potential electron acceptors for AOM were carried out in 2018 to investigate deeper the electron acceptors involved in CH_4 oxidation in the anoxic compartment of Lake Dendre, besides sulfate, which is available at high concentrations (>500 µmol L^{-1}) throughout the water column (Roland *et al.* 2017). These experiments revealed that NO_3^- addition significantly stimulated CH_4 oxidation at every depth from the oxic-anoxic interface down to 17 m. Furthermore, according to the stoichiometry of Equation 5 (see below, Jensen *et al.* 2009), measurement of CH_4 oxidation rates in control treatment (maximum of 3.8 CH_4 µmol L^{-1} d^{-1}) could fully sustain the natural denitrification rates measured (maximum of 2.9 N_2 µmol L^{-1} d^{-1}).

$$5CH_4 + 8NO_3^- + 8H^+ \rightarrow 5CO_2 + 4N_2 + 14H_2O \quad (5)$$

Jointly, these results could suggest a coupling between CH_4 oxidation and denitrification, which is thermodynamically favorable and has been widely reported in laboratory

Downloaded from https://academic.oup.com/femsec/article/97/10/fiab124/6360975 by University of Liege user on 17 September 2021

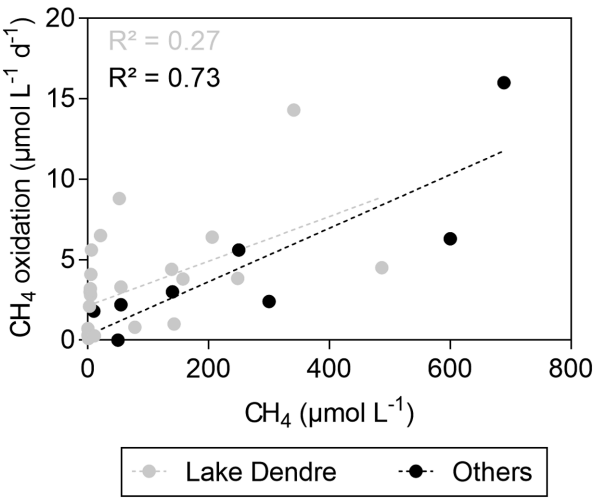

Figure 6. Methane oxidation rates (µmol L^{-1} d^{-1}) according to CH_4 concentrations (µmol L^{-1}), in Lake Dendre (gray) and in different lakes in the literature (black; see Table 1). The CH_4 oxidation rates in Lake Dendre are those observed during this study and during our previous study (Roland *et al.* 2017b).

experiments (e.g. Raghoebarsing *et al.* 2006; Ettwig *et al.* 2009). The in-situ occurrence of denitrification-dependent CH_4 oxidation in lakes has been mainly reported in sediments (Deutzmann and Schink 2011; á Deutzmann *et al.* 2014; Kojima *et al.* 2012; Liu *et al.* 2015; Norði and Thamdrup 2014), but to the best of our knowledge, only once in a lake water column (van Grinsven *et al.* 2020). In Lake Dendre, we hypothesize that the underwater spring supply the NO_3^- used to oxidize anaerobically a substantial part of the upward flux of CH_4. While SO_4^{2-} availability is sufficient throughout the entire water column and for the whole year (at least 500 µmol L^{-1}; Roland *et al.* 2017) to always sustain AOM, we speculate that the importance of NO_3^--dependent AOM varies seasonally in the function of the underwater spring discharge.

CH_4 oxidation rates also significantly increased with the addition of Fe oxides at every depth except 13 m (and may be due to competition with natural NO_3^- concentrations, which were high at this depth, NO_3^- being thermodynamically more favorable than Fe oxides for AOM; Borrel *et al.* 2011). By contrast, Mn addition did not significantly enhance CH_4 oxidation rates. The CH_4 oxidation coupled to Fe oxides in natural environments is still being investigated; it has been notably suggested to occur in Lake Matano (Indonesia; Crowe *et al.* 2011), Lake Orn (Denmark; á Norði *et al.* 2013), Lake Zug (Switzerland; Oswald *et al.* 2016), Lake La Cruz (Spain; Oswald *et al.* 2016a) or Siberian lakes (Cabrol *et al.* 2020). It could be of greater importance than originally expected (based on natural Fe oxide concentrations), because it has been estimated that Fe could be oxidized and reduced by 100 to 300 times before burial (Beal, House and Orphan 2009). Some studies also suggest that CH_4 oxidation stimulation by Fe oxides could be due to rapid oxidation of H_2S by Fe oxides, and then use of SO_4^{2-} formed for AOM (Segarra *et al.* 2015; Su *et al.* 2020). In Lake Dendre, SO_4^{2-} are large and not limiting (Roland *et al.* 2017), and thus it is quite unlikely that a relatively small supplemental supply of SO_4^{2-} increases the AOM rates. Nevertheless, iron is an important nutrient for many prokaryotes and we cannot exclude that a fraction of the Fe oxides added at the start of the incubations, if reduced to Fe^{2+}, might have stimulated AOM in alleviating a nutrient limitation. For instance, in culture experiments (Sub, Shuhei and Tanja 2012) or in marine ecosystems (Sivan *et al.* 2014), iron has been found to stimulate SO_4^{2-} reducers, and consequently SO_4^{2-}-driven AOM.

CONCLUSION

The results of this experiment, during which the addition of several electron acceptors was found to positively affect CH_4 oxidation, highlight that methanotrophy in the Lake Dendre water column seems to be diversified and would occur with different available potential electron acceptors. In this case, the availability of the different potential electron acceptors and the thermodynamics of the reactions would determine the magnitude and vertical segregation of the different processes, as suggested by the significant enhancement of CH_4 oxidation concomitant with the addition of electron acceptors (NO_3^-, Fe oxides). Furthermore, our results showed that, in addition to a linkage with the C cycle, the N cycle could also be linked to the sulfur S cycle, through chemolithotrophic denitrification using H_2S as the electron donor. This process could be particularly relevant in Lake Dendre, which is characterized by sulfate-rich waters throughout the water column and deep waters rich in H_2S (Roland *et al.* 2017).

Altogether, these results suggest that the microbial community involved in CH_4 oxidation was not specialized in the use of electron acceptors but was instead versatile, with an ability to use different substrates. We suggest the occurrence of several linkages between N, S and C cycles, notably between denitrification, anammox and sulfide oxidation, and CH_4 oxidation and denitrification. These results suggest that some processes are probably underestimated and underinvestigated in the literature, because the natural conditions are considered non-optimal for their occurrence.

FUNDING

This study was funded by the FNRS and the Walloon Institute of Sustainable Development WISD (contract X.3007.17).

SUPPLEMENTARY DATA

Supplementary data are available at *FEMSEC* online.

ACKNOWLEDGEMENTS

We thank Jean-Pierre Carlier and the members of the diving club 'Les Otaries' for their invaluable help in sampling. A.V.B. is research director at the Fonds National de la Recherche Scientifique (FNRS). C.M. and F.A.E.R. are post-doctoral researchers at the FNRS.

Conflict of interest. None declared.

REFERENCES

á Norði K, Thamdrup B, Schubert CJ. Anaerobic oxidation of methane in an iron-rich Danish freshwater lake sediment. *Limnol Ocean* 2013;**58**:546–54.

á Norði K, Thamdrup B. Nitrate-dependent anaerobic methane oxidation in a freshwater sediment. *Geochim Cosmochim Acta* 2014;**132**:141–50.

Abril G, Bouillon S, Darchambeau F *et al.* Technical Note: large overestimation of pCO2 calculated from pH and alkalinity in acidic, organic-rich freshwaters. *Biogeosciences* 2015;**12**:67–78.

Downloaded from https://academic.oup.com/femsec/article/97/10/fiab124/6360975 by University of Liege user on 17 September 2021

APHA. *Standard methods for the examination of water and wastewater*. American Public Health Association 1998.

Bai YN, Wang XN, Wu J *et al.* Humic substances as electron acceptors for anaerobic oxidation of methane driven by ANME-2d. *Water Res* 2019;**164**:114935.

Bar-Or I, Elvert M, Eckert W *et al.* Iron-coupled anaerobic oxidation of methane performed by a mixed bacterial-archaeal community based on poorly reactive minerals. *Environ Sci Technol* 2017;**51**:12293–301.

Barnard R, Leadley PW, Hungate BA. Global change, nitrification, and denitrification: a review. *Global Biogeochem Cycles* 2005;**19**:GB1007.

Bastviken D, Cole JJ, Pace ML *et al.* Fates of methane from different lake habitats: Connecting whole-lake budgets and CH_4 emissions. *J Geophys Res-Biogeo* 2008;**113**:G02024.

Bastviken D, Ejlertsson J, Tranvik L. Measurement of methane oxidation in lakes: A comparison of methods. *Environ Sci Technol* 2002;**36**:3354–61.

Battaglia G, Joos F. Marine N2O emissions from nitrification and denitrification constrained by modern observations and projected in multimillennial global warming simulations. *Global Biogeochem Cycles* 2018;**32**:92–121.

Beal EJ, House CH, Orphan VJ. Manganese-and iron-dependent marine methane oxidation. *Science* 2009;**325**:184–7.

Bernhard A. The Nitrogen Cycle: Processes, Players, and Human Impact. *Nat Educ Knowl* 2010;**3**:25

Blees J, Niemann H, Wenk CB *et al.* Micro-aerobic bacterial methane oxidation in the chemocline and anoxic water column of deep south-Alpine Lake Lugano (Switzerland). *Limnol Oceanogr* 2014;**59**:311–24.

Borges AV, Abril G, Darchambeau F *et al.* Divergent biophysical controls of aquatic CO_2 and CH_4 in the world's two largest rivers. *Sci Rep* 2015;**5**.

Borges AV, Darchambeau F, Lambert T *et al.* Effects of agricultural land use on fluvial carbon dioxide, methane and nitrous oxide concentrations in a large European river, the Meuse (Belgium). *Sci Total Environ* 2018;610–1.

Borrel G, Jézéquel D, Biderre-Petit C *et al.* Production and consumption of methane in freshwater lake ecosystems. *Res Microbiol* 2011;**162**:832–47.

Brettar I, Rheinheimer G. Denitrification in the Central Baltic: evidence for H2S-oxidation as motor of denitrification at the oxic-anoxic interface. *Marine Ecology Progress Series* 1991;**77**:157–69.

Cabrol L, Thalasso F, Gandois L *et al.* Anaerobic oxidation of methane and associated microbiome in anoxic water of Northwestern Siberian lakes. *Sci Total Environ* 2020;**736**:139588.

Capone DG, Kiene RP. Comparison of microbial dynamics in marine and freshwater sediments: contrasts in anaerobic carbon catabolism. *L&O* 1988;**33**:725–49.

Cole JJ, Caraco NF. Atmospheric exchange of carbon dioxide in a low-wind oligotrophic lake measured by the addition of SF6. *Limnol Oceanogr* 1998;**43**:647–56

Crowe SA, Katsev S, Leslie K *et al.* The methane cycle in ferruginous Lake Matano. *Geobiology* 2011;**9**:61–78.

Cui M, Ma A, Qi H *et al.* Anaerobic oxidation of methane: an "active" microbial process. *Microbiologyopen* 2015;**4**:1–11.

Dalsgaard T, Canfield DE, Petersen J *et al.* N2 production by the anammox reaction in the anoxic water column of Golfo Dulce, Costa Rica. *Nature* 2003;**422**:606–8.

Dalsgaard T, De Brabandere L, Hall Per OJ. Denitrification in the water column of the Central Baltic Sea. Geochim. *Cosmochim Acta* 2013;**106**:247–60.

Deutzmann JS, Schink B. Anaerobic oxidation of methane in sediments of Lake Constance, an oligotrophic freshwater lake. *Appl Environ Microbiol* 2011;**77**:4429–36.

Deutzmann JS, Stief P, Brandes J *et al.* Anaerobic methane oxidation coupled to denitrification is the dominant methane sink in a deep lake. *Proc Natl Acad Sci* 2014;**111**:18273 LP–18278.

Egger M, Rasigraf O, Sapart CJ *et al.* Iron-mediated anaerobic oxidation of methane in Brackish coastal sediments. *Environ Sci Technol* 2015;**49**:277–83.

Eller G, Känel L, Krüger M. Cooccurrence of aerobic and anaerobic methane oxidation in the water column of Lake Plußsee. *Appl Environ Microbiol* 2005;**71**:8925–8928.

Ettwig KF, Butler MK, Le Paslier D *et al.* Nitrite-driven anaerobic methane oxidation by oxygenic bacteria. *Nature* 2010;**464**:543–8.

Ettwig KF, Van Alen T, Van de Pas-Schoonen KT *et al.* Enrichment and molecular detection of denitrifying methanotrophic bacteria of the NC10 phylum. *Appl Environ Microbiol* 2009;**75**:3656–62.

Galán A, Faúndez J, Thamdrup B *et al.* Temporal dynamics of nitrogen loss in the coastal upwelling ecosystem off central Chile: evidence of autotrophic denitrification through sulfide oxidation. *L&O* 2014;**59**:1865–78.

Graf JS, Mayr MJ, Marchant HK *et al.* Bloom of a denitrifying methanotroph, 'Candidatus Methylomirabilis limnetica', in a deep stratified lake. *Environ Microbiol* 2018;**20**:2598–614.

IPCC. Climate change 2014: synthesis report. 2014.

Iversen N, Oremland RS, Klug MJ. Big Soda Lake (Nevada). 3. Pelagic methanogenesis and anaerobic methane oxidation. *Limnol Oceanogr* 1987;**32**:804–14.

Jensen MM, Kuypers MMM, Lavik G *et al.* Rates and regulation of anaerobic ammonium oxidation and denitrification in the Black Sea. *Limnol Oceanogr* 2008;**53**:23–36.

Jensen MM, Petersen J, Dalsgaard T *et al.* Pathways, rates, and regulation of N2 production in the chemocline of an anoxic basin, Mariager Fjord, Denmark. *Mar Chem* 2009;**113**:102–13.

Ji Q, Babbin AR, Jayakumar A *et al.* Nitrous oxide production by nitrification and denitrification in the Eastern Tropical South Pacific oxygen minimum zone. *Geophys Res Lett* 2015;**42**:10,710–755,764.

Kirchman DL, Sherr E, Sherr B *et al. Microbial Ecology of the Oceans*. John Wiley & Sons, NJ, USA 2008.

Kits KD, Klotz MG, Stein LY. Methane oxidation coupled to nitrate reduction under hypoxia by the Gammaproteobacterium Methylomonas denitrificans, sp. nov. type strain FJG1. *Environ Microbiol* 2015;**17**:3219–32.

Knittel K, Boetius A. Anaerobic oxidation of methane: progress with an unknown process. *Annu Rev Microbiol* 2009;**63**:311–34.

Kojima H, Tsutsumi M, Ishikawa K *et al.* Distribution of putative denitrifying methane oxidizing bacteria in sediment of a freshwater lake, Lake Biwa. *Syst Appl Microbiol* 2012;**35**:233–8.

Kuypers MMM, Lavik G, Woebken D *et al.* Massive nitrogen loss from the Benguela upwelling system through anaerobic ammonium oxidation. *PNAS* 2005;**102**:6478–83.

Labrenz M, Jost G, Pohl C *et al.* Impact of different in vitro electron donor/acceptor conditions on potential chemolithoautotrophic communities from marine pelagic redoxclines. *Appl Environ Microbiol* 2005;**71**:6664–72.

Liu Y, Zhang J, Zhao L *et al.* Aerobic and nitrite-dependent methane-oxidizing microorganisms in sediments of freshwater lakes on the Yunnan Plateau. *Appl Microbiol Biotechnol* 2015;**99**:2371–81.

Downloaded from https://academic.oup.com/femsec/article/97/10/fiab124/6360975 by University of Liege user on 17 September 2021

Lopes F, Viollier E, Thiam A *et al.* Biogeochemical modelling of anaerobic vs. aerobic methane oxidation in a meromictic crater lake (Lake Pavin, France). *Appl Geochem* 2011;**26**:1919–32.

Lu X, Bade DL, Leff LG *et al.* The relative importance of anammox and denitrification to total N2 production in Lake Erie. *J Great Lakes Res* 2018;**44**:428–35.

Oswald K, Graf JS, Littmann S *et al.* Crenothrix are major methane consumers in stratified lakes. *ISME J* 2017;**11**:2124–40.

Oswald K, Jegge C, Tischer J *et al.* Methanotrophy under versatile conditions in the water column of the ferruginous meromictic Lake La Cruz (Spain). *Front Microbiol* 2016a;**7**:1–16.

Oswald K, Milucka J, Brand A *et al.* Aerobic gammaproteobacterial methanotrophs mitigate methane emissions from oxic and anoxic lake waters. *Limnol Oceanogr* 2016b;**61**:S101–18.

Qin Y, Wu C, Chen B *et al.* Short term performance and microbial community of a sulfide-based denitrification and Anammox coupling system at different N/S ratios. *Bioresour Technol* 2019;**294**:122130.

Raghoebarsing AA, Pol A, Van de Pas-Schoonen KT *et al.* A microbial consortium couples anaerobic methane oxidation to denitrification. *Nature* 2006;**440**:918–21.

Reeburgh WS. Oceanic methane biogeochemistry. *Chem Rev* 2007;**107**:486–513.

Rissanen AJ, Karvinen A, Nykänen H *et al.* Effects of alternative electron acceptors on the activity and community structure of methane-producing and consuming microbes in the sediments of two shallow boreal lakes. *FEMS Microbiol Ecol* 2017;**93**:1–16.

Roland FAE, Darchambeau F, Borges AV *et al.* Denitrification, anaerobic ammonium oxidation, and dissimilatory nitrate reduction to ammonium in an East African Great Lake (Lake Kivu). *Limnol Oceanogr* 2018a;**63**:687–701.

Roland FAE, Darchambeau F, Morana C *et al.* Emission and oxidation of methane in a meromictic, eutrophic and temperate lake (Dendre, Belgium). *Chemosphere* 2017;**168**:756–64.

Roland FAE, Morana C, Darchambeau F *et al.* Anaerobic methane oxidation and aerobic methane production in an east African great lake (Lake Kivu). *J Great Lakes Res* 2018b;**44**:1183–93.

Rudd JWM, Hamilton RD, Campbell NER. Measurement of microbial oxidation of methane in lake water. *Limnol Oceanogr* 1974;**19**:519–24.

Saunois M, Bousquet P, Poulter B *et al.* The global methane budget: 2000-2012. *Earth System Science Data* 2016;**8**:697–751.

Saunois M, Stavert AR, Poulter B *et al.* The global methane budget 2000–2017. *Earth System Science Data* 2020;**12**:1561–623.

Scheller S, Yu H, Chadwick GL *et al.* Artificial electron acceptors decouple archaeal methane oxidation from sulfate reduction. *Science* 2016;**351**:703–7.

Schubert CJ, Durisch-Kaiser E, Wehrli B *et al.* Anaerobic ammonium oxidation in a tropical freshwater system (Lake Tanganyika). *Environ Microbiol* 2006;**8**:1857–63.

Schubert CJ, Vazquez F, Lösekann-Behrens T *et al.* Evidence for anaerobic oxidation of methane in sediments of a freshwater system (Lago di Cadagno). *FEMS Microbiol Ecol* 2011;**76**:26–38.

Segarra KEA, Schubotz F, Samarkin V *et al.* High rates of anaerobic methane oxidation in freshwater wetlands reduce potential atmospheric methane emissions. *Nat Commun* 2015;**6**:7477.

Sivan O, Adler M, Pearson A *et al.* Geochemical evidence for iron-mediated anaerobic oxidation of methane. *Limnol Oceanogr* 2011;**56**:1536–44.

Sivan O, Antler G, Turchyn A V *et al.* Iron oxides stimulate sulfate-driven anaerobic methane oxidation in seeps. *Proc Natl Acad Sci* 2014;**111**:E4139–47.

SPW-DGO3. Etat des nappes d'eau souterraine de Wallonie. *Belgique* 2021;1–66.

Sturm A, Fowle DA, Jones C *et al.* Rates and pathways of CH_4 oxidation in ferruginous Lake Matano, Indonesia. *Biogeosciences Discuss* 2016;**2016**:1–34.

Sturm A, Fowle DA, Jones C *et al.* Rates and pathways of CH_4 oxidation in ferruginous Lake Matano, Indonesia. *Geobiology* 2019;**17**:294–307.

Su G, Zopfi J, Yao H *et al.* Manganese/iron-supported sulfate-dependent anaerobic oxidation of methane by archaea in lake sediments. *Limnol Oceanogr* 2020;**65**:863–75.

Sub SM, Shuhei O, Tanja B. Effects of iron and nitrogen limitation on sulfur isotope fractionation during microbial sulfate reduction. *Appl Environ Microbiol* 2012;**78**:8368–76.

Thamdrup B, Dalsgaard T, Jensen MM *et al.* Anaerobic ammonium oxidation in the oxygen-deficient waters off northern Chile. *Limnol Oceanogr* 2006;**51**:2145–56.

Thamdrup B, Dalsgaard T. Production of N_2 through anaerobic ammonium oxidation coupled to nitrate reduction in marine sediments. *Appl Environ Microbiol* 2002;**68**:1312–8.

Valenzuela EI, Padilla-Loma C, Gómez-Hernández N *et al.* Humic substances mediate anaerobic methane oxidation linked to nitrous oxide reduction in wetland sediments. *Front Microbiol* 2020;**11**:587.

Valenzuela EI, Prieto-Davó A, López-Lozano NE *et al.* Anaerobic methane oxidation driven by microbial reduction of natural organic matter in a tropical wetland. *Appl Environ Microbiol* 2017;**83**. https://doi.org/doi:10.1128/AEM.00645-17.

van Grinsven S, Sinninghe Damsté JS, Abdala Asbun A *et al.* Methane oxidation in anoxic lake water stimulated by nitrate and sulfate addition. *Environ Microbiol* 2020. https://doi.org/doi:10.1111/1462-2920.14886.

Weiss RF, Price BA. Nitrous oxide solubility in water and seawater. *Mar Chem* 1980;**8**:347–59.

Weiss RF. Determinations of carbon dioxide and methane by dual catalyst flame ionization chromatography and nitrous oxide by electron capture chromatography. *J Chromatogr Sci* 1981;**19**:611–6.

Wenk CB, Blees J, Zopfi J *et al.* Anaerobic ammonium oxidation (anammox) bacteria and sulfide-dependent denitrifiers coexist in the water column of a meromictic south-alpine lake. *Limnol Oceanogr* 2013;**58**:1–12.

Westwood D. Ammonia in waters. In: HMSO(ed) *Methods for the examination of waters and associated materials*. Stationery Office Books, London, UK 1981.

Yamamoto S, Alcauskas JB, Crozier TE. Solubility of methane in distilled water and seawater. *J Chem Eng Data* 1976;**21**:78–80.

Downloaded from https://academic.oup.com/femsec/article/97/10/fiab124/6360975 by University of Liege user on 17 September 2021